Low-abundant but highly transcriptionally active uncharacterised Nitrosomonas drive ammonia-oxidation in the Brouage mudflat, France

Fabien Cholet, Hélène Agogué, Umer Z Ijaz, Nicolas Lachaussée, Philippe Pineau, Cindy J Smith

Science of the Total Environment 946 (2024) 174312

Contents lists available at ScienceDirect

Science of the Total Environment

journal homepage: www.elsevier.com/locate/scitotenv

Low-abundant but highly transcriptionally active uncharacterised *Nitrosomonas* drive ammonia-oxidation in the Brouage mudflat, France

Fabien Cholet [a,*], Hélène Agogué [b], Umer Z. Ijaz [a], Nicolas Lachaussée [b], Philippe Pineau [b], Cindy J. Smith [a]

[a] Advanced Research Centre, Infrastructure and Environment, James Watt School of Engineering, University of Glasgow, 11 Chapel Lane G11 6EW, Glasgow, UK.
[b] LIENSs, UMR 7266, CNRS - La Rochelle Université, 2 Rue Olympe de Gouges, 17000, La Rochelle, France

HIGHLIGHTS

- Higher nitrification rates in runnels despite higher AOB abundance in ridges.
- Low-abundant *Nitrosomonas* dominate transcriptionally active community.
- High-abundant *Nitrosospira/Nitrosomonas* were transcriptionally dormant.
- Abundance of transcriptionally active *Nitrosomonas* correlates with PNR.
- Nitrification is driven by <5 % of the total AOB community.

GRAPHICAL ABSTRACT

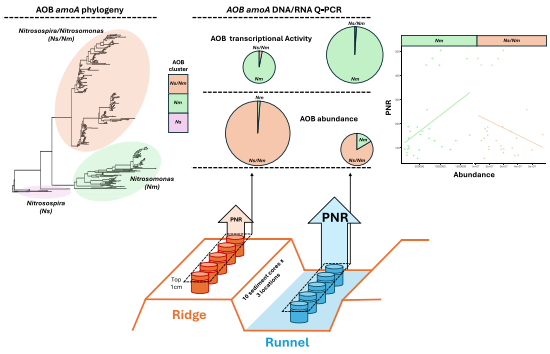

ARTICLE INFO

Editor: Frederic Coulon

Keywords:
Nitrification
amoA
amoA transcripts
Coastal sediments

ABSTRACT

Exploring differences in nitrification within adjacent sedimentary structures of ridges and runnels on the Brouage mudflat, France, we quantified Potential Nitrification Rates (PNR) alongside *amoA* genes and transcripts. PNR was lower in ridges (≈1.7 fold-lower) than runnels, despite higher (≈1.8 fold-higher) ammonia-oxidizing bacteria (AOB) abundance. However, AOB were more transcriptionally active in runnels (≈1.9 fold-higher). Sequencing of *amoA* genes and transcripts revealed starkly contrasting profiles with transcripts from ridges and runnels dominated (≈91 % in ridges and ≈98 % in runnels) by low abundant (≈4.6 % of the DNA community in runnels and ≈0.8 % in ridges) but highly active phylotypes. The higher PNR in runnels was explained by higher abundance of this group, an uncharacterised *Nitrosomonas sp.* cluster. This cluster is phylogenetically similar to other active ammonia-oxidizers with worldwide distribution in coastal environments indicating its potential, but previously overlooked, contribution to ammonia oxidation globally. In contrast DNA profiles were dominated by highly abundant but low-activity clusters phylogenetically distinct from known *Nitrosomonas (Nm)* and *Nitrosospira (Ns)*. This cluster is also globally distributed in coastal sediments, primarily detected as DNA, and often classified as *Nitrosospira* or *Nitrosomonas*. We therefore propose to classify this cluster as *Ns/Nm*. Our work indicates that low abundant but highly active AOB could be responsible for the nitrification globally, while the abundant AOB *Ns/Nm* may not be transcriptionally active, and as such account for the lack of correlation

* Corresponding author.
E-mail address: Fabien.Cholet@glasgow.ac.uk (F. Cholet).

https://doi.org/10.1016/j.scitotenv.2024.174312
Received 9 April 2024; Received in revised form 3 June 2024; Accepted 24 June 2024
Available online 25 June 2024

between rate processes and gene abundances often reported in the literature. It also raises the question as to what this seemingly inactive group is doing?

1. Introduction

Coastal bays are crucial ecosystems providing economic and ecological services (Costanza et al., 2014). Human activities heavily impact them, leading to increased pollution runoff including excess nitrogen loading (Agardy et al., 2005; Seitz et al., 2014). High concentrations of nitrogen cause eutrophication, eventually leading to water column anoxia (Gruber and Galloway, 2008). Microbial denitrification and anaerobic ammonia oxidation (ANAMMOX) play pivotal roles in mitigating nitrogen by converting nitrite/nitrate to gaseous forms (Damashek et al., 2015; Hou et al., 2012). Biological nitrification, the chemo-litho-autotrophic oxidation of ammonia to nitrate, plays a central role as it controls available substrate for denitrification and ANAMMOX (Seitzinger et al., 2006). The first step of nitrification, ammonia oxidation (AO), is carried out by both archaea (ammonia-oxidizing archaea; AOA) and bacteria (ammonia-oxidizing bacteria; AOB), while COMAMMOX *Nitrospira* oxidize ammonia to nitrite and then nitrate in a single organism (Daims et al., 2016; Daims et al., 2015; van Kessel et al., 2015). Besides its importance for the remediation of excess nitrogen loading, AO is also relevant in the context of environmental greenhouse gas production. AO directly leads to the production of N_2O, *via* nitrifier-denitrification (ND), and the incomplete oxidation of hydroxylamine, an obligate intermediate in the ammonia oxidation pathway of both AOA and AOB (Kool et al., 2011; Prosser et al., 2020). AO is indirectly responsible for N_2O production by denitrifying microbes, through the generation of nitrite and nitrate (Prosser et al., 2020). In this context, understanding who the active ammonia oxidizing microbes (AOM) are in natural and engineered environments and what key parameters control their activity is essential.

While ammonia oxidation is one of the most studied microbial processes, reflected by the *amoA* gene being the second most frequently sequenced gene after *16S ribosomal RNA* (Alves et al., 2018), the connection between AO rates and the structure, abundance, and activity of the AOM community is not always clear, likely due to the fact that the majority of published research focusses on abundance alone. This is particularly evident from the number of studies that use the difference in abundance between AOA and AOB to extrapolate whether bacteria or archaea are driving the nitrification process (Bernhard et al., 2007; Caffrey et al., 2007; Chang et al., 2017; Li et al., 2015; Marton et al., 2015; Mosier and Francis, 2008; Sanders and Laanbroek, 2018; Santoro et al., 2008; Smith et al., 2015; Wankel et al., 2011). The major limitation of this approach is that it postulates that all ecotypes within a community are active and oxidize ammonia at the same rate. The latter assumption is clearly refuted by studies of AOA and AOB pure cultures (Dimitri Kits et al., 2017) as well as observations in natural environments that rates correlate to the presence of key taxa rather than the size of the overall community (Alves et al., 2013; Bernhard et al., 2007; Duff et al., 2017; Santos et al., 2018). In comparisons, the first assumption has rarely been tested but targeted transcriptomics of AOM communities frequently report lower numbers of *amoA* transcripts (RNA) compared to the number of *amoA* genes (DNA) for the same sample (Bowen et al., 2014; Duff et al., 2017; Fan et al., 2015; He et al., 2018; Li et al., 2022; Lipsewers et al., 2014; Liu and Yang, 2021; Marshall et al., 2023; Tatti et al., 2022; Urakawa et al., 2014; Zhang et al., 2018; Zhang et al., 2015a; Zhang et al., 2015b). This indicates either an overall low transcriptional activity of the AOM communities as on average less than one *amoA* mRNA is produced per *amoA* gene or that only a fraction of the AOM community is active at any given moment. The latter explanation is supported by the few studies that compared total and transcriptionally active community composition in coastal sediments. Zhang et al. (2018) using time-series incubations with and without acetylene, not only examined total and active AOM communities across a soil-sediment gradient but for AOB from sediments, showed a series of active AOB phylotypes from transcripts that were not present in corresponding DNA. Similarly, but from *in situ* sediments across a bay, Duff et al. (2017) recovered several AOB *amoA* clones from mRNA libraries that were not present at DNA level and were phylogenetically distinct from the dominant DNA *amoA*. Finally, Tatti et al. (2022), this time exploring the active AOM responding in sediment PNR incubations, showed the presence of several AOB *amoA* phylotypes from transcripts that were not detected in DNA profiles. While these studies used relatively low-resolution approaches, they strongly suggested the presence of low-abundant but high activity AOB members.

The above studies indicate that the dominant AOB at gene level may not be driving nitrification but instead low abundant highly active AOB are. Here we explore this hypothesis using the unique adjacent sedimentary structures on the Brouage intertidal mudflat (France). This site is characterised by the presence of ridges (elevations) and runnels (depressions) on the middle part of the mudflat. These natural semi-permanent structures are formed and maintained by differences in sedimentation dynamics and the bio-stabilisation effect of the extracellular polymeric substance (EPS) produced by the microphytobenthos in ridges (Blanchard et al., 2000). Previous studies have shown that the microbial communities in the Brouage mudflat exhibit strong stratification influenced by salinity, nutrients, and meiofauna (Lavergne et al., 2017) rather than by diel and tidal rhythms (Lavergne et al., 2018). More importantly, significant differences in both actual and potential nitrification rates have been evidenced between adjacent ridges and runnels with higher rates measured in runnels (Laima et al., 2002; Laima et al., 1999) and these differences are likely not explained by differences in AOM community composition (Cholet et al., 2022). We hypothesise that these differences will be explained by both a higher overall abundance of AOM in runnels and by a higher proportion of transcriptionally active taxa, and directly compare DNA and mRNA *amoA* profiles to explore the role of low-abundant *versus* dominant taxa in driving nitrification.

2. Material and methods

2.1. Site description and sampling

The Marenne-Oléron bay covers an area of 180 km^2 on the French Atlantic coast, in-between Oléron Island and the mainland. On the middle part of the Brouage mudflat ridges are formed by sedimentation events rather than being residual structures resulting from the carving of runnels from a flat mud formation (Carling et al., 2009) (Supplementary Fig. 1). Three sites spanning the ridge-runnel structure of the Brouage mudflat were sampled at low tide (North station-N, VASIREMI station-V and south station-S) on the 1st, 2nd and 3rd of July 2019 (Fig. 1A). At each station, 5 individual ridge/runnel structures were sampled (replicates 1 to 5), at least 5 m distant from each other. Each replicate consisted of 5 cores (top 1 cm) along the same ridge/runnel at ≈2 m intervals and homogenised by mixing.

2.2. Biological and physiochemical analyses

Nutrients concentrations were determined from pore water extracted by centrifugation and filtration through 0.2 μm cellulose nitrate filters using a SEAL AA3 autoanalyzer (Seal Analytical, GmbH Nordertedt, Germany) as described in Bergeon et al. (2023). Salinity and pH were measured directly on unfiltered pore water. Sediment Total Organic Carbon (TOC) was determined by weight loss of samples incubated at

450 °C for 12 h. Sediment density was determined by weight loss weight of samples incubated at 60 °C for 48 h. Sediment granulometry was measured on a Mastersizer laser granulometer 2000 with a Hydro MU sampler (Malvern Panalytical, UK). Chlorophyll a and phaeopigments (*i.e.,* concentration of degraded chlorophyll pigment) concentrations were quantified by fluorimetry according to the protocol of Lorenzent (1966). Sediment prokaryotic cells were quantified by flow cytometry using a 2-extractions protocol previously described in Lavergne et al. (2014).

2.3. Potential nitrification rates (PNR)

Potential nitrification rates (PNR) were measured using fresh sediments incubated in artificial seawater supplemented with 24 μM NaN_3 and 0 μM or 250 μM of $(NH_4)_2SO_4$. After 24 h, the accumulation of nitrite was determined by subtraction the initial nitrite concentration (see biological and physiochemical analyses and Supplementary Material and Methods).

2.4. DNA/RNA extraction, RNA quality check, reverse transcription and Q-PCR

DNA and RNA were extracted using the RNeasy PowerSoil RNA kit with the RNeasy PowerSoil DNA elution kit (Qiagen; UK). RNA fractions were further DNase treated using the Turbo DNase Kit (Ambion; UK) to ensure the absence of DNA carryover. Total RNA integrity was evaluated by calculating the RIN using the Bioanalyser 2100 RNA Nano (Agilent Technologies; UK) and messenger RNA (mRNA) integrity was evaluated using the ratio amplicon approach (Cholet et al., 2019) (R_{amp}). DNA-free RNA was used for complementary DNA (cDNA) synthesis using Superscript IV (SSIV) kit (Invitrogen; UK) using gene specific (GS) primers (Cholet et al., 2020). *16S rRNA* genes were amplified using primers described in Suzuki et al. (2000) and the iTaq Universal Probes Supermix (Bio-Rad; UK) and functional genes and transcripts were quantified from the DNA and cDNA, respectively, by quantitative PCR using primers described in Hornek et al. (2006) (AOB *amoA*) and Wuchter et al. (2006) (AOA *amoA*) and the QuantiTech SYBR Green kit (Qiagen;

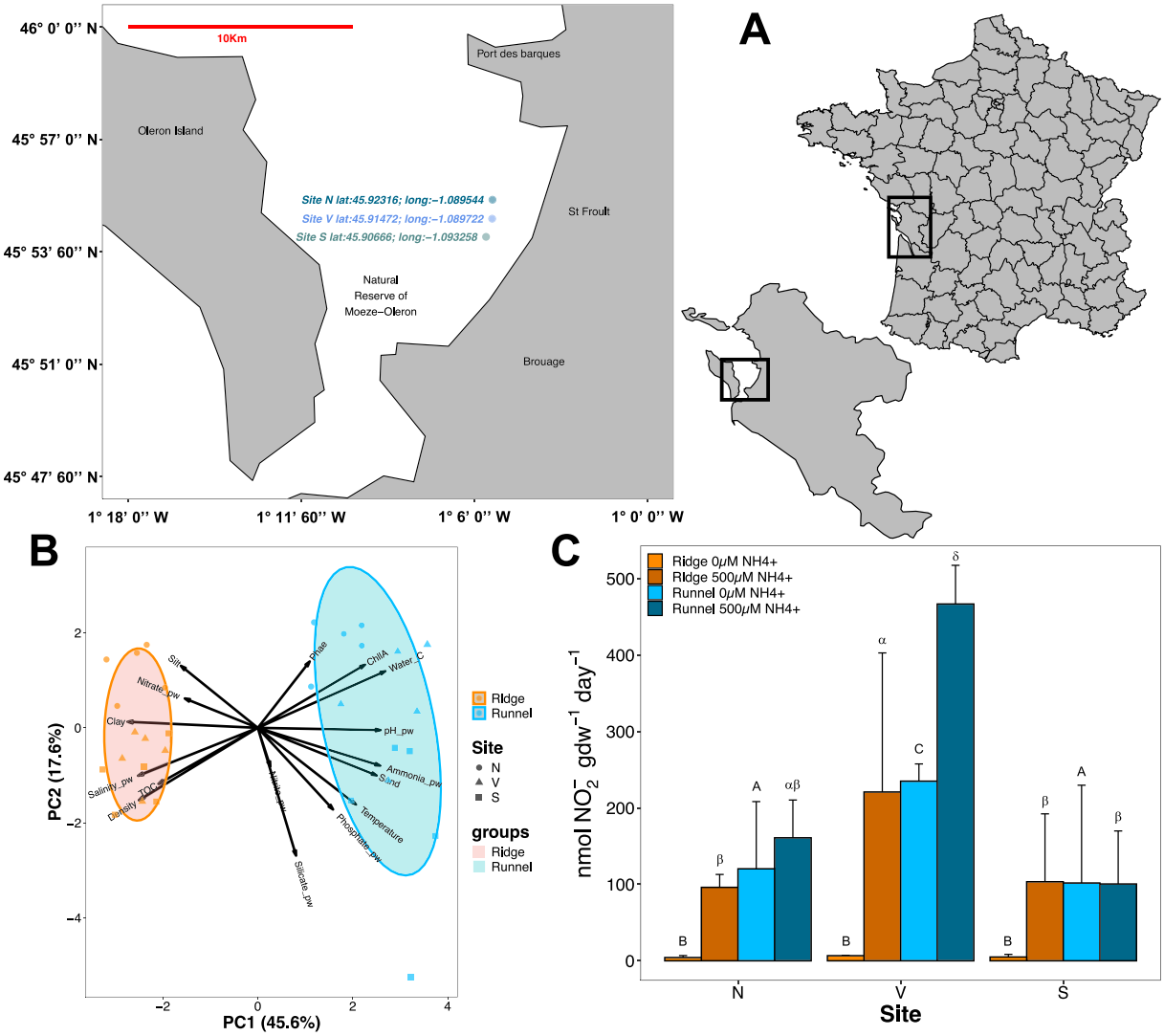

Fig. 1. The ridge and runnel structures of the Brouage mudflat, French Atlantic coast. Mudflat location along the French Atlantic coast where three separate sites of ridge-runnel structures with the bay were sampled (A), each with significantly different physiochemical conditions (B) and Potential Nitrification rates (C). "pw": parameter measured on pore water; Water_C: water content; TOC: Total Organic Carbon; ChlA: Chlorophyll a; phae: phaeopigments; CN.pw: Total Carbon/ Total Nitrogen ratio in pore water. ProK_abund: Prokarotes abundance measured by flow cytometry. Maps A and B were made using the `ggmap` package (Kahle and Wickham, 2013). For sample identification N, V and S refer to the North, VASIREMI and South stations, respectively; B/S for the sediment structure (B for ridges and S for runnels) and biological replicates are number 1 to 5. For PNR, differences between ridges and runnels and sampling sites were tested by two-way ANOVA and post-hoc TuckeyHSD tests (separately for PNR with and without ammonia amendment). Statistically significant differences are represented by letters on top of the boxplots; different letters indicate statistically different means (p-value<0.05).

UK) (Table 1).

2.5. Illumina MiSeq amplicon libraries preparation and processing of high-throughput sequencing (HTS) data

Amplicon sequencing library for Illumina MiSeq HTS sequencing (300 Paired-End; 22 million reads/lane) was prepared as described previously in Cholet et al. (2019) using primers listed in Table 1. For *16S rRNA,* ASVs (Callahan et al., 2017) were constructed using the DADA2 pipeline (Callahan et al., 2016). For functional genes, ASV construction and sequence quality check was carried out following the guidelines for functional genes described in Cholet et al. (2022) (R scripts available at https://github.com/Fchlt/ARC). The phylogeny proposed by Alves et al. (2018) was used as reference database for AOA *amoA*. For AOB *amoA*, a new reference database was generated (Supplementary material and methods).

2.6. Statistical analysis

All statistical analyses were carried out in R. A zero-centred and variance-scaled physicochemical data matrix was used as input for PCA using the prcomp function from the stats package (R Core Team, 2021, https://www.R-project.org/). PCA was visualised using the ggbiplot function from the ggplot2 package (Wickham, 2016). Overall differences in physiochemical parameters between ridges and runnels and sites were then tested using a two-way permutational multivariate analysis of variance (PERMANOVA) using the adonis2 function from the vegan package (Oksanen et al., 2005) and the Euclidian distance matrix as input. Differences in individual physiochemical parameters between ridges and runnels and sites were also tested using a two-way analysis of variance (ANOVA). Gene/transcript copy number values were normalised per grams of sample (dry weight; gdw^{-1}) while PNR values were normalised per grams of sample and per day of incubation (gdw^{-1} day^{-1}). Differences between ridges and runnels and sampling sites were tested using two-ways analysis of variance (ANOVA) using the aov function from the stats package.

For HTS data analysis of *16S rRNA* and AOB *amoA*, absolute ASV abundances were inferred from the high-throughput sequencing data and Q-PCR quantification as described in Tettamanti Boshier et al. (2020) and Jian et al. (2020). For AOA *amoA*, rarefied abundance tables were used as Q-PCR results from the RNA extraction were too low. Differences in community composition were tested by PERMANOVA using the Bray-Curtis, Unifrac and Weighted Unifrac (WUnifrac) phylogenetic distances between samples. Differential abundance analysis between ridges and runnels was carried out using analysis of composition of microbes with bias correction (ANCOM-BC Lin and Peddada, 2020). Further details are provided in the Supplementary material and methods.

3. Results

3.1. Ridges and runnels have differing physio-chemical environments, with higher ammonia and potential nitrification rates (PNR) in the runnels

Ridges and runnels separated clearly based on measured environmental parameters (Fig. 1B, Table 2), with 44.5 % of the variance explained by PC1. 14.6 % of the variance (PC2), separated site N (more positive values along PC2) from sites V and S (more negative values along PC2). Ridges had finer and drier sediments, were slightly more acidic, with a higher salinity, total organic carbon, but lower ammonia, phosphate, photosynthetic pigments and prokaryotes concentration than runnels. Runnels were characterised by four times higher ammonia concentration, higher photosynthetic pigments, and higher prokaryotes concentration (Table 2).

Higher PNR was measured in runnels (120.3 ± sd = 44; 235 ± 11.3 and 101.8 ± 64 nmol NO_2^- $.gdw^{-1}.day^{-1}$ at site N, V and S, respectively)

Table 1
List of primers and PCR conditions used in this study.

Primer	Sequence (5'→3')	Orientation	Target (length)	PCR cycle conditions	Q-PCR			Reference (Primer sequences)
					Slope/ Efficiency	Intercept	R^2	
BacamoA-1F	GGGGHTTYTACTGGTGGT	Forward	Bacterial *amoA* gene (491 bp)	PCR: 95 °C-15 min; [94 °C-30s; 47 °C(DNA) or 55 °C(cDNA) -30s; 72 °C-30s]x32; 72 °C-10 min	cDNA: -3.94/ 79.39 %	cDNA: 41.02 DNA: 41.8	cDNA: 0.995 DNA: 0.999	Hornek et al. (2006)
BacamoA-2R	CCCCTCBGSAAAVCCTTCTTC	Reverse		Q-PCR: 95 °C-15 min; [95 °C-30s; 47 °C(DNA) or 55 °C(cDNA)-30 s; 72 °C-1 min; 79.5 °C-2 s plate read]x40; melt curve 65°→95°; 0.5° increment/ 5 s	DNA: -4.07/ 76.08 %			
Arch-amoWAF	CTGAYTGGGCYTGGACATC	Forward	Archaeal *amoA* gene (256 bp)	PCR: 95 °C-15 min; [95 °C-30s; 58 °C-40s, 72 °C-1 min]x35; 72 °C-10 min	−4.46/ 67.58 %	43.97	0.999	Wuchter et al. (2006)
Arch-amoWAR	TTCTTCTTTGTTGTGCCCAGTA	Reverse		Q-PCR: 95 °C-15 min; [95 °C-30s; 58 °C-40s, 72 °C-10s + plate read]x40; melt curve 65°→95°; 0.5° increment/ 5 s				
Nisp-162F	GGATTTCTGGNTSGATTGGA	Forward	COMAMMOX *Nitrospira clade A/B amoA* (197 bp)	95 °C-15 min; 40×(94 °C-30s; 48 °C-30s; 72 °C-1 min + plate read); melt curve 65°→95°; 0.5° increment/ 5 s	−4.28/ 71.26 %	43.43	0.999	Fowler et al. (2018)
Nisp-359R	WAGTTNGACCACCASTACCA	Reverse						
515F	GTGYCAGCMGCCGCGGTAA	Forward	Bacterial/Archeal *16S rRNA* (V4-V5; 411 bp)	PCR: 95 °C-15 min; [94 °C-45 s, 50 °C-30s, 72 °C-40s]x25; 72 °C-10 min	NA			Walters et al. (2015)
926R	CCGYCAATTYMTTTRAGTTT	Reverse						
1369F	CGGTGAATACGTTCYCGG	Forward	Bacterial/Archeal *16S rRNA* (V9; 123 bp)	Q-PCR: 95 °C-10 min; [95 °C-10s, 60 °C-30s + plate read]x40; 40 °C-10 min	−3.25/ 103.09 %	39.87	0.989	Suzuki et al. (2000)
1492R	GGWTACCTTGTTACGACTT	Reverse						
1389P	CTTGTACACACCGCCCGTC	Probe						

Table 2
Environmental parameters measured in ridges and runnels.

Parameter	Mean Ridges ±sd	Mean Runnels ±sd	Structure	Site
Salinity.pw (‰)	36.47 ± 1.12	33.81 ± 0.66	***	***
pH.pw	7.02 ± 0.08	7.21 ± 0.06	***	***
Nitrate.pw (μM)	1.56 ± 1.2	0.7 ± 0.18	**	*
Nitrite.pw (μM)	0.07 ± 0.03	0.07 ± 0.02	–	–
Ammonia.pw (μM)	44.1 ± 15.49	203.89 ± 85.87	***	–
Phosphate.pw (μM)	0.07 ± 0.05	0.13 ± 0.09	**	***
Silicate.pw (μM)	163.27 ± 21.36	176.19 ± 37.37	–	***
Water.C (%)	43.36 ± 1.64	50.62 ± 2.23	***	–
TOC (%)	14.79 ± 2.62	10.89 ± 2.43	***	–
Chl *a* (μg/g)	10.32 ± 3.12	20.13 ± 6.24	***	–
Phae (μg/g)	15.39 ± 1.6	20.72 ± 9.3	*	***
Prokaryotes (cells.ml^{-1})	$6.6 \times 10^6 \pm 8.5 \times 10^5$	$7.0 \times 10^6 \pm 1.3 \times 10^6$	–	–
16S rRNA (copies g^{-1})	$7.93 \times 10^9 \pm 3.58 \times 10^9$	$1.08 \times 10^{10} \pm 6.21 \times 10^9$	*	***
CN.pw	5.9 ± 0.53	2.96 ± 0.96	***	–
Sand (%)	7.82 ± 1.03	14.51 ± 3.95	***	–
Silt (%)	81.14 ± 1.76	78.22 ± 3.67	*	–
Clay (%)	11.04 ± 1.19	7.27 ± 0.81	***	–

pw: parameters measured on pore water; Water.C: water content; TOC: Total Organic Carbon; Chl *a*: Chlorophyll *a*; Phae: phaeopigments; CN.pw: Total Carbon/ Total Nitrogen ratio in pore water. Prokaryotes cell numbers measured by flow cytometry. Results of two-way ANOVAs testing the effect of the sediment structure and sampling site are presented on the right: - no difference; p * < 0.05;** < 0.01;*** < 0.001.

compared to ridges (4.27 ± 1.3; 6.7 ± 0.2 and 4.9 ± 1.7 nmol NO_2^- . gdw^{-1}.day^{-1} at site N, V and S, respectively) (p-value <0.001, Fig. 1C). Sampling site also had a significant effect (p-value site<0.01). PNR remained significantly higher in runnels for the incubation with 500 μM ammonia added (160.9 ± 24.7 and 466.7 ± 25.3 nmol NO_2^- .gdw^{-1}. day^{-1} at sites N and V, respectively) compared to ridges (96.1 ± 8.4 and 220.8 ± 91 nmol NO_2^- .gdw^{-1}.day^{-1} at sites N and V, respectively) but the differences at site S were no longer significant (100.5 ± 34.7 and 103.4 ± 44.4 nmol NO_2^- .gdw^{-1}.day^{-1} in runnels and ridges, respectively) (Fig. 1C).

3.2. Bacterial abundance and communities differ between ridges and runnels

16S rRNA gene abundances were significantly higher in runnels than ridges (p-value = 0.0221) (Table 2). Sediment structures also had a significant effect on the overall microbial community based on *16S rRNA* gene sequencing, (p-value <0.001 for all three phylogenetic distances, Bray-Curtis, Unifrac and Weighted Unifrac) with 5.7 % Bray-Curtis, 13.8 % Unifrac and 33.7 % Weighted Unifrac variance in the microbial community composition explained by the ridge/runnel structures (Supplementary Fig. 3, Supplementary Table 2).

3.3. Ammonia oxidizers gene abundance is higher in ridges but transcripts are higher in runnels

AOB *amoA* gene abundances were higher in ridges ($3.81 \times 10^7 \pm 1.17 \times 10^7$ copies .gdw^{-1}) than runnels ($2.09 \times 10^7 \pm 5.27 \times 10^6$ copies .gdw^{-1}) (0.01 > p-value >0.001). Sampling site was not statistically significant, with comparable values within ridges ($3.63 \times 10^7 \pm 1.01 \times 10^7$; $4.58 \times 10^7 \pm 1.17 \times 10^7$ and $3.18 \times 10^7 \pm 1.01 \times 10^7$ copies . gdw^{-1}at sites N, V and S, respectively) and within runnels at all sites ($1.97 \times 10^7 \pm 3.67 \times 10^6$; $2.16 \times 10^7 \pm 7.92 \times 10^6$ and $2.14 \times 10^7 \pm 4.27 \times 10^7$ copies .gdw^{-1} at sites N, V and S, respectively) (Fig. 2; Supplementary Table 3). Interesting, the opposite trend was seen in AOB *amoA* transcript abundance, which were, on average, higher in runnels ($3.29 \times 10^6 \pm 3.29 \times 10^6$ copies .gdw^{-1}) than ridges ($1.66 \times 10^6 \pm 8.84 \times 10^5$ copies .gdw^{-1}) (0.01 > p-value >0.001). (Fig. 2; Supplementary Table 3) although only significantly higher at site N ($8.21 \times 10^6 \pm 4.09 \times 10^6$ copies .gdw^{-1} in runnels) (p-value>0.01). Within ridges, AOB *amoA* transcripts abundances were similar between sites ($1.92 \times 10^6 \pm 1.13 \times 10^6$; $1.34 \times 10^6 \pm 4.70 \times 10^6$ and $1.78 \times 10^6 \pm 1.07 \times 10^6$ copies .gdw^{-1} at sites N, V and S, respectively) and comparable to values in runnels at sites V ($2.00 \times 10^6 \pm 5.45 \times 10^5$ copies .gdw^{-1}) and S ($1.63 \times 10^6 \pm 4.03 \times 10^5$ copies .gdw^{-1}). Transcription ratio of bacterial *amoA* DNA:RNA was <1 at all sites, with significantly higher ratio of

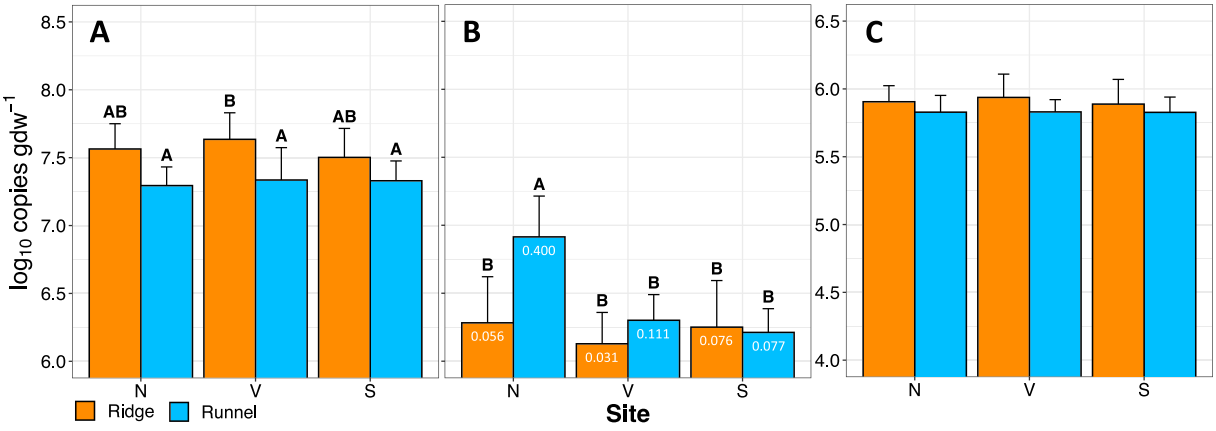

Fig. 2. AOM abundance and transcriptional activity in ridges and runnels. AOB *amoA* DNA (A), AOB *amoA* RNA (B) and AOA *amoA* DNA (C). Numbers reported as log10 transformed copies per gram of sediment (dry weight). For AOB *amoA* RNA, transcription ratios are reported inside barplots. Differences between ridges and runnels and sampling sites were tested by two-ways ANOVA and post-hoc TuckeyHSD tests. Statistically significant differences are represented by letters on top of the barplots; different letters indicate statistically different means (p-value<0.05).

transcripts to DNA in runnels (0.196 ± 0.177) compared to ridges (0.052 ± 0.023) (p-value <0.001) (Fig. 2; Supplementary Table 3). Within runnels, a higher ratio was found at site N (0.400 ± 0.188) compared to sites V (0.111 ± 0.065) and S (0.077 ± 0.087) whereas the ratio within ridges was relatively constant between sampling sites (0.052 ± 0.022; 0.030 ± 0.011 and 0.076 ± 0.020 at site N, V and S, respectively) (Fig. 2; Supplementary Table 3). AOA *amoA* genes abundances were lower than AOB, but showed the same pattern of higher numbers in ridges ($8.22 \times 10^5 \pm 1.87 \times 10^5$ copies .gdw^{-1}) than runnels ($6.74 \times 10^5 \pm 9.00 \times 10^4$ copies .gdw^{-1}) ($0.05 > p$-value >0.01) (Fig. 2; Supplementary Table 3). AOA *amoA* transcripts could not be reliably quantified by Q-PCR with melt curve analysis showing multiple peaks indicating possible unspecific amplification (Supplementary Fig. 4). As there were $\approx 10^5$ copies .gdw^{-1} in DNA we assumed there must be some transcriptional activity and therefore combined and concentrated three separate PCRs of the cDNA to obtain sufficient product for sequencing (supplementary material and methods). Finally, COMAMMOX *Nitrospira amoA* gene copies were quantified at low concentrations ($2.5 \times 10^4 \pm 4.9 \times 10^3$ and $2.9 \times 10^4 \pm 1.9 \times 10^3$ copies .gdw^{-1} in runnels and ridges at site V) however, despite the assay and standard curve amplification working well, the melt curve analyses of the environmental assays indicated unspecific amplification, concluding that COMAMMOX was below the reliable detection limits of our assay (Supplementary Fig. 4).

3.4. Ammonia oxidiser community composition- different phylotypes dominate the total (DNA) and transcriptionally active (RNA) communities

Although AOA *amoA* transcripts were too low for quantification, amplicons were recovered for sequencing by pooling three separate PCR reactions. For both AOA and AOB, most of the variance was explained by the differences between the DNA and RNA libraries (p-value<0.01; $R^2 =$ 0.942 and 0.782 for AOB and AOA, respectively). The overall effect of the ridge/runnel structures was also significant for both AOB and AOA (PERMANOVA p-value<0.01) but explained a much smaller part of the variance ($R^2 = 0.018$ and 0.058 for AOB and AOA, respectively) (Fig. 3A and D). When the DNA and RNA libraries were analysed separately, the effect of the ridge/runnel structures became more important for both AOA and AOB (p-value<0.01), with R^2 values of 0.467 and 0.435 for AOB (DNA and RNA, respectively; Fig. 3B and C) and 0.485 and 0.339 for AOA (DNA and RNA, respectively; Fig. 3E and F). Overall, these results indicated a definitive difference between the total and transcriptionally active AOM communities as well as a significant effect of the ridge/runnel structures on total and transcriptionally active AOA and AOB.

3.4.1. Ammonia oxidizing archaea

In total, 1359 AOA *amoA* ASVs were recovered from the sequencing of the DNA and RNA libraries after quality filtering. The AOA community was dominated by the *Nitrosopumilales-Gamma-2.1* group, representing ≈96 % and ≈97 % of the total AOA community in ridges and runnels, respectively. The second most abundant group was the closely related *Nitrosopumilales-Gamma-2.2*, representing ≈3.7 % and ≈2.6 % of the total AOA community in ridges and runnels, respectively. Other *Nitrosopumilales* groups belonging to the *Nitrosopumilales Gamma*, *Delta* and *Epsilon* were present in ridges and runnels but together represented ≈0.1 % of the total community. *Nitrosopumilales -Eta* and *-Zeta* were also present, only in ridges, albeit at a marginally low relative abundance (>0.005 %) (Fig. 4B; Supplementary Table 4). Within the *Nitrosopumilales-Gamma-2.1*, the total AOA community was dominated by ASV_1 (28 % in ridges and 34 % in runnels), ASV_2 (25 % in ridges and 19 % in runnels), ASV_3 (11 % in ridges and 10 % in runnels) and ASV_4 (3 % in ridges and 4 % in runnels) whose closest known AOA were *Nitrosopumilus cobalaminigenes* (ASV_1) and *Nitrosopumilus sediminis* (ASV_2/3/4) (Fig. 4A, Supplementary Table 5). ANCOM-BC test revealed that numerous individual ASVs were over-represented (*i.e.* more abundant) in either the ridges or runnel. This included the abundant ASV_2, over-represented in ridges (25 % in ridges and 18.5 % in runnels) in addition to several ASVs belonging to the *Nitrosopumilales Delta* and *Epsilon* groups (Supplementary Table 6), while in the runnels, ASVs belonging to the *Gamma* groups were over-represented (Fig. 4D, Supplementary Table 6). The profile of the AOA community changed when considering the actively transcribing community, with a relative ≈16 fold increase in the proportion of *Nitrosopumilales-Gamma-2.2*

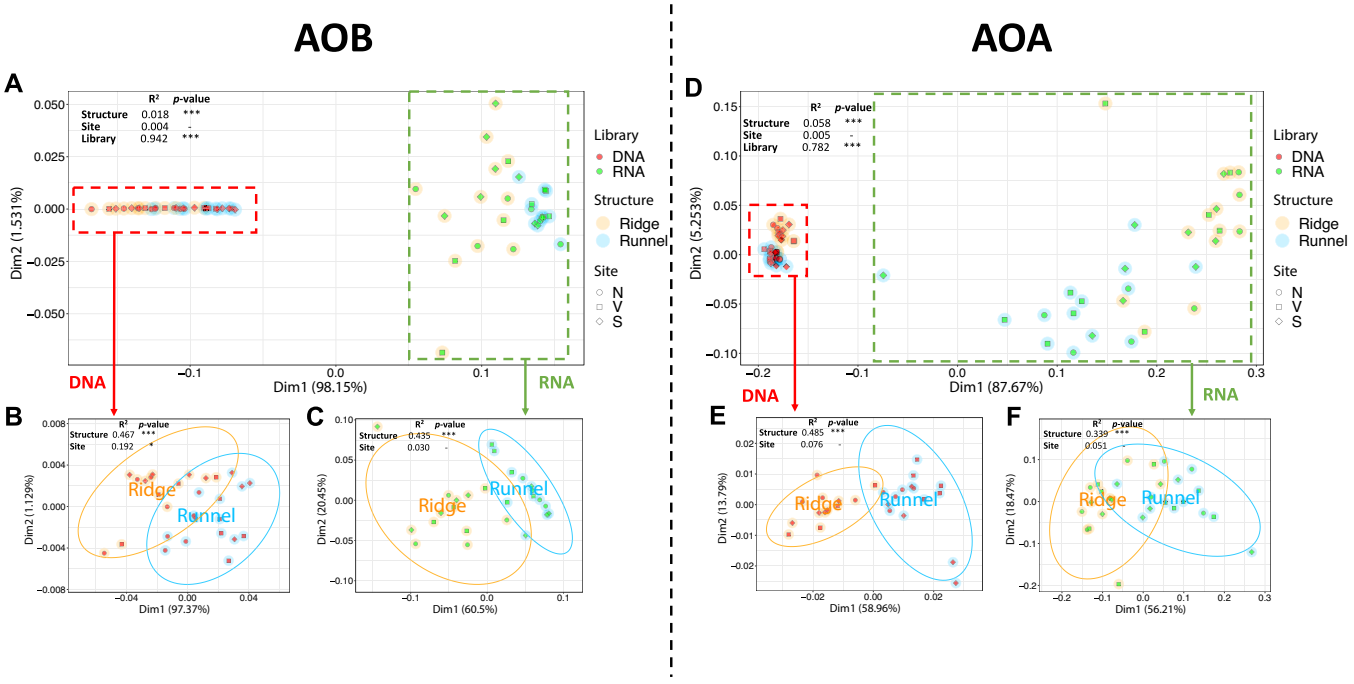

Fig. 3. Differences in total and transcriptionally active AOM communities in ridges and runnels. PCoA plots show differences in AOB (A, B and C) and AOA (D, E and F) communities, considering DNA and RNA analysis together (A and D), DNA only (B and E) or RNA only (C and F). p-values and R^2 values reported are the results of two-ways (or three-ways for A and D) PERMANOVA tests. - no difference; p * < 0.05 ** <0.01 *** < 0.001.

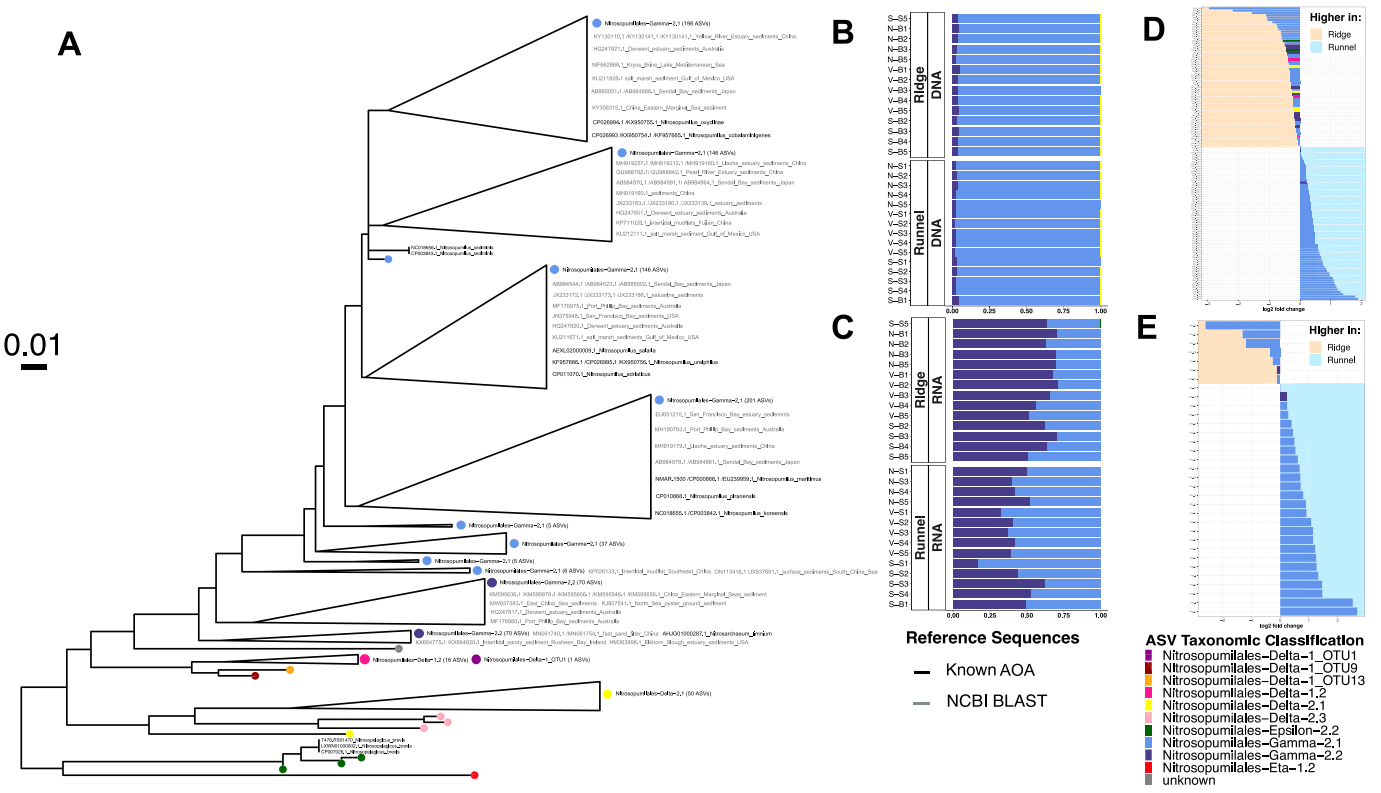

Fig. 4. Comparative analysis of AOA communities in ridges and runnels. A) Visualization of the phylogenetic relationships among AOA *amoA* ASVs from this study (coloured circles), reference *amoA* sequences from known AOA (black tip labels) and AOA *amoA* sourced from the NCBI database (grey tip labels). ASV taxonomy from this study is displayed at the bottom right of the Fig. B) and C) Quantification of the relative abundance of AOA *amoA* ASVs in DNA and RNA libraries, respectively. D) and E) Differential abundance analysis highlighting individual ASVs (Y-axis) with significantly different representation between ridges (negative log2 fold change values on the X-axis) and runnels (positive log2 fold change values on the X-axis) in the DNA and RNA libraries, respectively. ASV taxonomy is color-coded consistently with the legend on the phylogenetic tree.

compared to the DNA community (≈64 % in ridges and ≈43 % in runnels) and in turn a relative decrease (≈2.7 and ≈1.7 fold in ridges and runnels, respectively) in the proportion of *Nitrosopumilales-Gamma-2.1* (≈36 % in ridges and ≈57 % in runnels) (Fig. 4B and C; Supplementary Table 4). *Nitrosopumilales-Epsilon-2.2* were also detected in ridges (≈0.4 %) but not in runnels. The differential abundance analysis at RNA level revealed that a small number of transcriptionally active AOA ASVs (n = 22) were differentially represented between ridges and runnels and the majority belonged to the *Gamma-2.1* group (Fig. 4E; Supplementary Table 6).

3.4.2. *Ammonia oxidizing bacteria- the majority of environmental AOB amoA in the reference database cannot be assigned to either Nitrosomonas or Nitrosospira*

AOB *amoA* sequences in the reference database clustered in three main phylogenetic groups. Two groups could be identified as the *Nitrosomonas* (n = 1792) and *Nitrosospira* (n = 402) lineages as they contained representative sequences from known *Nitrosomonas* and *Nitrosospira*, respectively, along with environmental sequences. The third and largest group (n = 3382), composed of environmental sequences only, formed a distinct cluster that contained sequences designated as *Nitrosospira*-like by Francis et al. (2003) and O'Mullan and Ward (2005) and as *Nitrosomonas Cluster Group A* and *Cluster Group* B by Zhang et al. (2018) and Duff et al. (2017) (Supplementary Fig. 2). Based on the absence of obvious phylogenetic relationship between this cluster and known AOB species and the confusion in its naming in the literature, we propose to classify these sequences as a separate *Nitrosospira/Nitrosomonas* (*Ns/Nm*) cluster. Within each of the three main clusters, subclusters sharing respective unique common ancestors (except for *Ns/Nm A*) and supported by bootstrap values >50 were defined. (Supplementary Fig. 2).

3.4.3. *Ammonia oxidizing bacteria- phylogenetic classification of ASVs*

In total, 478 AOB *amoA* ASVs were recovered from DNA and RNA libraries after quality filtering and separated in three main clusters. Two clusters could be clearly identified as *Nitrosomonas* (128 ASVs) and *Nitrosospira* (10 ASVs) based on their phylogenetic relationship with known AOB species. The third largest cluster, primarily composed of DNA sequences, contained 344 ASVs taxonomically assigned to the newly defined *Ns/Nm Group A* (179 ASVs) and *Ns/Nm Group B* (165 ASVs). Sequences in the *Ns/Nm* cluster were phylogenetically related to DNA and RNA amplicons from Irish coastal sediments (Duff et al., 2017; Zhang et al., 2018). On the DNA tree (Fig. 5A), separation between the *Nitrosospira* cluster and the rest of the tree was supported by a bootstrap value of 100 and the separation between the *Nitrosomonas* and *Ns/Nm* clusters was supported by a bootstrap value of 99. Overall, the AOB *amoA* nucleotide tree was consistent with the amino acid tree, except that on the amino acid tree, the *Nitrosospira* cluster and *Ns/Nm* cluster share a common ancestor not shared by the *Nitrosomonas* cluster (Supplementary Fig. 5).

The *Nitrosomonas cluster* branched into 4 subclusters with 2 subclusters of known *Nitrosomonas*. The first one contained 7 ASVs assigned to the *Nitrosomonas nitrosa* lineage and 1 to the *Nitrosomonas europaea/halophila/eutropha/communis* lineage. This cluster also contained reference *amoA* sequences from *Nitrosomonas nitrosa, Nitrosomonas eutropha, Nitrosomonas europeae, Nitrosomonas halophila, Nitrosomonas communis and Nitrosomonas cryotolerans.* The second subcluster of known *Nitrosomonas* contained 1 ASV assigned to the *Nitrosomonas oligotropha/ureae/supralitoralis* lineage and 1 ASV assigned to the *Nitrosomonas marina/aestuarii* lineage as well as reference *amoA* sequences from

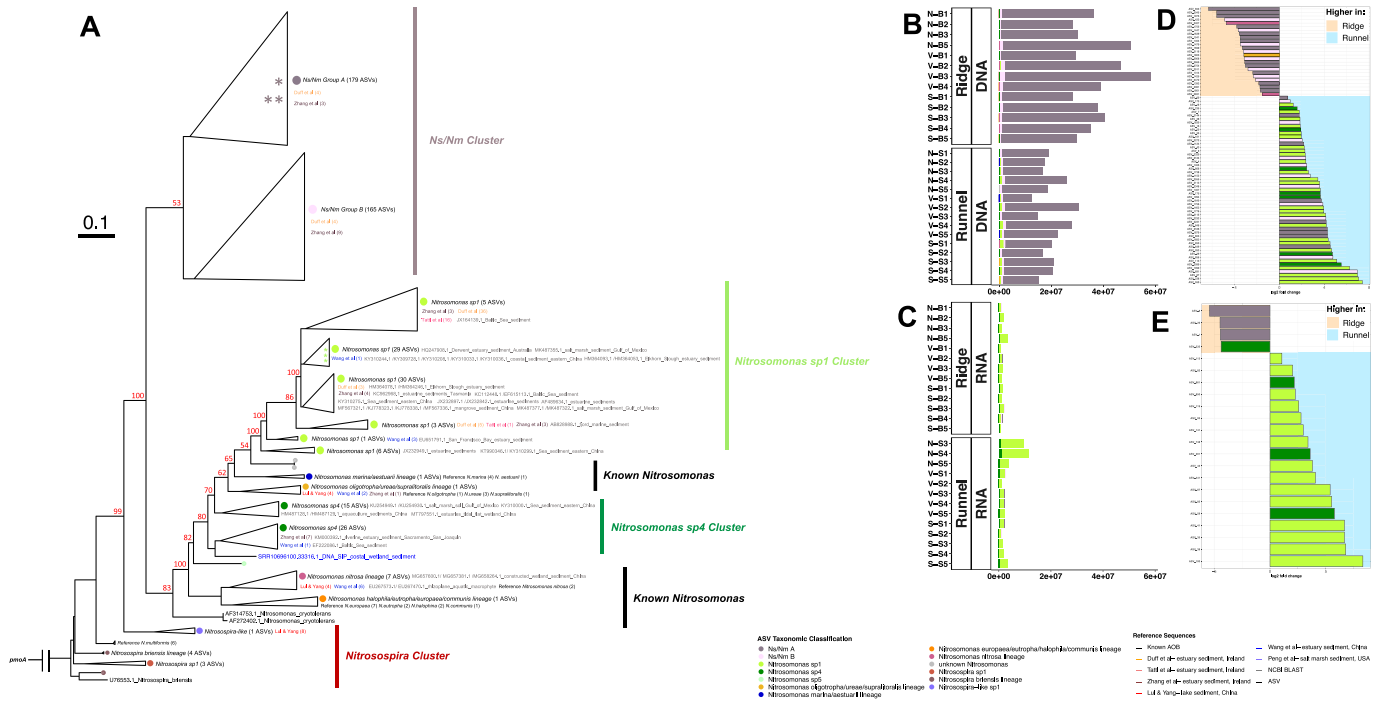

Fig. 5. Comparative analysis of AOB communities in ridges and runnels. A) Visualization of the phylogenetic relationships among AOB *amoA* ASVs from this study (coloured circles), reference *amoA* sequences from known AOB (black tip labels), AOB *amo*A sourced from literature libraries (coloured tip labels; see legend for source study) and AOB *amoA* sourced from the NCBI database (grey tip labels). ASV taxonomy from this study is displayed at the bottom right of the Fig. The beige and green stars show the position of the dominant ASVs at DNA (ASV_1/2/3) and RNA (ASV_4/6/7) levels, respectively. B) and C) Quantification of the absolute abundance of AOB *amoA* ASVs in DNA and RNA libraries, respectively. D) and E) Differential abundance analysis highlighting individual ASVs (Y-axis) with significantly different representation between ridges (negative log2 fold change values on the x-axis) and runnels (positive log2 fold change values on the X-axis) in the DNA and RNA libraries, respectively. ASV taxonomy is color-coded consistently with the legend on the phylogenetic tree.

Nitrosomonas marina, *Nitrosomonas aestuarii, Nitrosomonas urea*, *Nitrosomonas oligotropha* and *Nitrosomonas supralitoralis.* Both clusters contained RNA *amoA* sequences from freshwater sediment, China (Wang et al., 2020). The majority of actively transcribing AOB, were found in two clusters and in particular in the *Nitrosomonas sp1 cluster* (76 ASVs), which branched separately from the known *Nitrosomonas,* with other active AOB from coastal environments, including, RNA amplicons from Irish coastal sediments (Duff et al., 2017; Tatti et al., 2022; Zhang et al., 2018), DNA SIP amplicons from coastal wetlands, China (Wang et al., 2020) as well as DNA sequences from coastal and estuary sediments across the globe (*e.g.* Baltic sea, eastern China, Gulf of Mexico, San Francisco Bay, Elkhorn Slough estuary). The remaining smaller *Nitrosomonas Clusters sp4 cluster*, contained 41 ASVs related to RNA amplicons from Irish coastal sediments (Zhang et al., 2018) and DNA SIP amplicons from coastal wetlands (Wang et al., 2020). One ASV was identified as *Nitrosomonas sp5* and 2 ASVs could not be assigned to one of the *denovo* clusters (designated unknown *Nitrosomonas*). Finally, a *Nitrosospira* cluster of 10 ASVs was present (in the DNA library only), related to RNA *amoA* sequences from freshwater lake sediments, China (Liu and Yang 2021) (Fig. 5A; Supplementary Fig. 5).

3.4.4. Ammonia oxidizing bacteria cluster ns/nm dominates the total (DNA) community while Nitrosomonas sp1 and sp4 dominate the transcriptionally active (RNA) community

In both ridges and runnels, the total AOB community (DNA library) was dominated by ASVs from *Cluster Ns/Nm Group A* (≈97 % and ≈92 % of the reads in ridges and runnels, respectively) with three ASVs representing ≈70 % of the read (ASV_1 and ASV_2 and AVS_3 representing ≈28 %, ≈ 22 % and ≈23 % in ridges and ≈23 %, ≈ 24 % and ≈22 % in runnels, respectively). *Cluster Ns/Nm Group B* was the second most abundant phylotype in ridges (≈2.6 %) followed by *Nitrosomonas sp1* (≈0.8 %) while in runnels, *Nitrosomonas sp1* was more abundant than *Ns/Nm Group B* (4.6 % and 3.1 %, respectively). Interestingly, *Nitrosomonas sp1* was also 3-fold more abundant in runnels compared to ridges when considering absolute abundances (9.5×10^5 and 3.2×10^5 reads in runnels and ridges, respectively). *Nitrosomonas sp4*, *sp5*, known *Nitrosomonas* and *Nitrosospira* together accounted for only ≈0.04 % and ≈0.1 % of the community in ridges and runnels, respectively. *Nitrosomonas sp4* was ≈3.7 and ≈1.8 fold more abundant in runnels than ridges when considering relative and absolute abundances, respectively. Differential abundance analysis showed that, out of the 53 ASVs that were significantly more abundant in runnels, 26 belonged to *Nitrosomonas sp1* and 7 to *Nitrosomonas sp4*, while out of the 25 ASVs significantly more abundant in the ridges, 14 belonged to the *Ns/Nm Cluster Group A*, 8 to the *Ns/Nm Cluster Group B,* 2 to the *Nitrosomonas nitrosa* lineage and 1 to the *Nitrosomonas oligotropha/ureae/supralitoralis* lineage (Fig. 5; Supplementary Table 7 and 8).

In sharp contrast to the DNA profile, at RNA level, *Nitrosomonas sp1 and sp4* ASVs were the most abundant actively transcribing AOB, accounting for ≈91 % of ridge and ≈99 % of runnel reads. Within this group, *Nitrosomonas sp1* was dominant (78 % in ridges and 88 % in runnels). Three *Nitrosomonas sp1* ASVs, (ASV_4, ASV_6 and ASV_7,) represented ≈28 %, ≈11 % and ≈10 % of the reads in ridges and ≈34 %, ≈15 % and ≈10 % of the reads in runnels. *Nitrosomonas sp4* was the second most transcriptionally active cluster accounting for ≈13 % in ridges and ≈11 % in runnels and was dominated by a single ASV (ASV_11), representing ≈9 % of ridges and runnels. When considering absolute abundances, *Nitrosomonas sp1* and *Nitrosomonas sp4* were ≈3.3 and ≈2.3 fold more transcriptionally active in runnels than ridges, respectively. Differential abundance analysis showed that 18 ASVs were significantly more transcriptionally active in runnels than ridges and they all belonged to the *Nitrosomonas* clusters (15 ASVs from *Nitrosomonas sp1* and 3 ASVs from *Nitrosomonas sp4*). Only 1 ASV from *Nitrosomonas sp4* was more active in ridges. The dominant ASVs at RNA

level (ASV_4 and ASV_6) were on average more transcriptionally active in runnels than in ridges but the differential analysis revealed this was not statistically significant. *Ns/Nm Cluster A/B*, which dominated the DNA library, only accounted for ≈9 % and ≈0.8 % of the reads in ridges and runnels, respectively. Differential abundance analysis identified 3 ASVs belonging to the *Ns/Nm Goup A*, which were significantly more transcriptionally active in ridges than runnels (Fig. 5; Supplementary Table 7, 8 and 9).

4. Discussion

4.1. Differences in nitrification rates between ridges and runnels are likely driven by low-abundance high-activity uncharacterised Nitrosomonas clusters

To determine which AOM drive the nitrification process in the Brouage mudflat, AOA and AOB abundances and transcriptional activities were measured. While AOA genes could be quantified, AOA *amoA* transcripts were present in very low abundance as revealed by inconclusive Q-PCR melt curves (Supplementary Fig. 4) and the need for three individual end-point PCRs to recover enough cDNA for sequencing. Similarly, COMAMMOX *Nitrospira amoA* genes abundance was ≈3.5 orders of magnitude lower than that of AOB *amoA* and analyses of Q-PCR melt curves indicated possible unspecific amplifications (Supplementary Fig. 4). In contract, AOB genes abundances and transcripts were higher ($>10^7$ and $> 10^6$ copies .gdw^{-1} for AOB *amoA* genes and transcripts, respectively) and reliably quantified from all samples. From these observations, we concluded that AOB were likely the main drivers of ammonia oxidation. To quantify the differences in the maximum potential of ridges and runnels to oxidize ammonia, potential nitrification rates were further employed as this approach has been shown previously to be adequate in mud sediments dominated by AOB, with the same phylotypes active *in-situ* and during the PNR incubations (Tatti et al., 2022). A quantitative comparison of the phylotypes found in the total and transcriptionally active AOB communities revealed that the ammonia oxidation within the Brouage mudflat is not driven by the abundant *Ns/Nm cluster*, who dominated the AOB community, as this phylotype was transcriptionally inactive and was more abundant in ridges where lower PNR was measured. Instead, we hypothesise that the ammonia oxidation is driven by uncharacterised *Nitrosomonas sp* phylotypes who dominated the transcriptionally active AOB community. Despite only representing a small portion (>5 %) of the total AOB community, the abundance of this phylotype was on average three times higher in runnels and positively correlated with PNR (Supplementary Fig. 6). To further test this hypothesis, rate per cell were calculated, only considering the absolute abundance of *Nitrosomonas sp1* and *sp4* and 2.5 copies of *amoA* per genomes. This yielded values of 3.55 and 38.67 fmol NH_4^+ .cell^{-1} .h^{-1} for the PNR without ammonia amendment in ridges and runnels, respectively and 93.30 and 66.60 fmol NH_4^+ .cell^{-1} .h^{-1} for the PNR with ammonia amendment in ridges and runnels, respectively. These estimated values are higher than that reported by Wang et al. (2020) for AOB in soil and sediments (3.38 to 16.93 fmol NH_4^+ .cell^{-1}. h^{-1}) and by Su et al. (2018) for AOB in constructed wetlands sediments (0.02 to 10.37 fmol NH_4^+ .cell^{-1} .h^{-1}) as well as those determined for cultures of AOB (0.9 to 53 fmol of NH_4^+ .cell^{-1} .h^{-1}) (Coskuner et al., 2005). It should be noted that Su et al. (2018) used total AOB abundance, assuming each cell is active, rather than the specific abundance of the active AOB population, likely overestimating the number of active cells. Meanwhile, the number of active AOB cells calculated here are likely underestimated by using *in situ* abundances rather than the abundance in the PNR incubation. Nevertheless, these values are within the same order of magnitude as those previously reported indicating that it is theoretically possible that *Nitrosomonas sp1* and *sp4* are solely responsible for driving the ammonia oxidation process in the Brouage mudflat.

Overall, results presented here together with previous observations (Duff et al., 2017; Tatti et al., 2022; Zhang et al., 2018) suggest that in some sediments, only a subset of the total AOB communities drives the nitrification process. Similar observations were made for AOA with strong difference between the DNA and RNA profiles. While not being the main driver of the ammonia-oxidation process here, it indicates that low-abundance AOA might also be highly transcriptionally active. Differences between total and transcriptionally active AOM have been observed in other environments, suggesting that low-abundance AOM might play important roles elsewhere, while the abundant phylotypes are not always transcriptionally active. When comparing the effect of allylthiourea (ATU) exposure on soil AOA and AOB communities, He and Ji (2020) showed that one AOB clusters, representing ≈50 % of the total community in ATU exposed samples was completely absent from the transcriptionally active community. Inversely, they showed the presence of two low-abundance *Nitrosomonas* Clusters representing 0.006 % and 0.003 % of the total community that were highly active, accounting for 10.9 % and 13.1 % of the transcriptionally active community. Similarly, Liu et al. (2022), who studied the abundance and activity of AOA in coastal water, reported that the AOA cluster WCB, which represented 50 % of the total community at one non-upwelling station, was completely absent in the corresponding RNA sample. Meanwhile, the AOA cluster SCM1-like which accounted for a high proportion at RNA level at the upwelling stations was found at very low abundance in corresponding DNA samples. Taken together with results presented here, these observations indicate an important role of low-abundant AOM in ammonia oxidation. In this context, we argue that quantitative transcriptional activity should routinely complement DNA based studies in order to bridge the gap between community composition, active organisms, and rate process.

In turn, these fundings also raise the very interesting question as to what the abundant *Ns/Nm* AOB DNA cluster is doing if they are not actively transcribing the ammonia monooxygenase gene? The sequences from this numerically dominate cluster, were reassigned to a new unified group that we have called the *Ns/Nm* cluster as they fall between and therefore do not share a strong phylogenetic relationship with known *Nitrosomonas* or *Nitrospira*. As there are no known cultured representative of this group (Supplementary Fig. 5), speculations as to the metabolic capacities of this phylotype that enable it to be so abundant are difficult to make. One possible explanation is that they may be able to grow mixotrophically, using organic compounds as carbon and energy source as might be the case for some other AOM (Wright and Lehtovirta-Morley, 2023; Hommes et al., 2003).

4.2. Biogeographical distribution of Nitrosomonas clusters in coastal/estuary sediments

In this study, we illustrate the importance of integrating measures of transcriptional activity alongside abundance data. Failing to do so would have resulted in a flawed comprehension of ammonia oxidation in the Brouage mudflat, prompting us to question whether this discrepancy reflects a global trend. The *Nitrosomonas sp1 and sp4* phylotypes have previously been recovered as active AOM from other coastal (Duff et al., 2017; Tatti et al., 2022; Zhang et al., 2018;' Peng et al., 2012; Wang et al., 2020) and freshwater environments (Liu and Yang 2021) (Fig. 5A; Fig. 6; Supplementary Fig. 5), indicating they could be a significant contributor to nitrification in other coastal ecosystems. To determine their broader biogeographical distribution in coastal environments, the *denovo* AOB clusters defined from the reference database were segregated by geographical origin. We found that *Nitrosomonas sp1 and sp4* are detected in the majority of studies and are broadly distributed across the globe. In some studies, a high proportion of sequences recovered belonged to these clusters (Fig. 6). Since most studies used clone libraries to assess community composition, finding a high proportion of *Nitrosomonas sp1* and *sp4* clones indicate that they may represent a much higher proportion of the total community in those samples compared to the samples from the Brouage mudflat. This

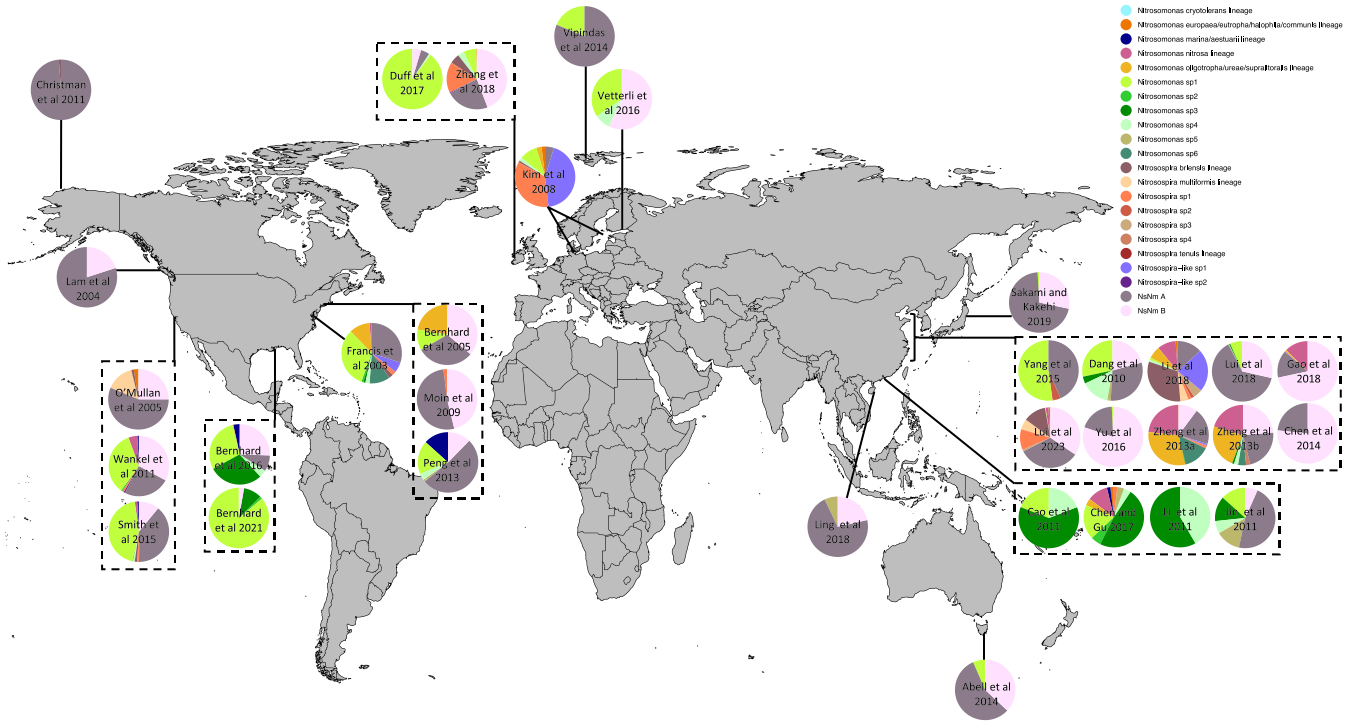

Fig. 6. Biogeographical distribution of AOB clusters in coastal sediments. Pie charts represent the proportion of clones or ASVs (Lui et al. 2023) assigned to the *denovo* AOB clusters in each study. Reference studies are indicated for inside each pie charts.

observation could indicate that they play a key role in ammonia oxidation in coastal sediments worldwide. The *Ns/Nm* AOB clusters are also found in almost all studies and often constitute the majority of *amoA* sequences recovered. The studies considered here (Fig. 6) were undertaken at DNA level, and correlations between gene abundances and rates are not always found, raising the question as to which group are driving nitrification. The evidence we have derived from a French coastal sediment in the present study and evidence from similar environments on the Irish west coast (Duff et al., 2017; Tatti et al., 2022; Zhang et al., 2018) indicates similar scenario, where low-abundant AOB display high transcriptional activity and are potentially responsible for driving nitrification.

Broad biogeographical studies involving measures of abundance, community composition and transcriptional activity, coupled with rate process, are needed to answer the questions raised by the results presented here: Are *Nitrosomonas sp1* and *sp4* always low in abundance and highly active in coastal sediments? Here we were able to explain differences in PNR at the meter-scale within the same mudflat by the differences in abundance of these clusters but can the same apply at larger geographical scale (*i.e.* regional, continental)? And furthermore, why is there a highly abundant seemingly inactive *Ns/Nm* cluster? Is the *Ns/Nm cluster* active in other samples and if not, how can we explain their high abundance?

5. Conclusions

We show that the higher PNR in runnels compared to ridges can be explained by the higher abundance of uncharacterised low-abundance high-activity *Nitrosomonas* clusters in runnels, that are the active phylotypes in both ridges and runnels. These cluster have a broad geographical distribution indicating their importance for ammonia oxidation in coastal/estuary sediments worldwide. Discrepancies between PNR and overall AOB abundance are explained by the presence of a low-activity AOB cluster that is more abundant in ridges but does not participate in the ammonia oxidation process. This low-activity AOB cluster is phylogenetically distinct from known *Nitrosomonas* and *Nitrosospira* and is also broadly distributed in coastal/estuary sediments worldwide. Future work should routinely include quantitative transcriptomics, not as a replacement of DNA based methods but rather as a complementary approach. Combining these methods with high throughput sequencing and rate measurement, future research should test if the patterns of activity found here are observed at broader geographical scales and what physiochemical parameters regulates active AOM globally. Finally, results obtained from the sequencing of short amplicons will always be limited in their reach. Consequently, efforts at cell isolation directly from the environment as well as genome reconstruction are also needed in order to determine the metabolic capacities of different AOM phylotypes.

CRediT authorship contribution statement

Fabien Cholet: Writing – review & editing, Writing – original draft, Visualization, Validation, Supervision, Software, Resources, Project administration, Methodology, Investigation, Funding acquisition, Formal analysis, Data curation, Conceptualization. **Hélène Agogué:** Writing – review & editing, Validation, Supervision, Resources, Project administration, Methodology, Investigation, Conceptualization. **Umer Z. Ijaz:** Software, Resources. **Nicolas Lachaussée:** Resources, Methodology. **Philippe Pineau:** Resources, Methodology. **Cindy J. Smith:** Writing – review & editing, Visualization, Validation, Supervision, Resources, Project administration, Methodology, Investigation, Funding acquisition, Conceptualization.

Declaration of competing interest

The authors declare the following financial interests/personal relationships which may be considered as potential competing interests:

Fabien Cholet reports financial support was provided by Microbiology Society. Cindy Smith reports financial support was provided by Science Foundation Ireland Starting Investigator Award. Cindy Smith reports financial support was provided by Royal Academy of Engineering. Cindy Smith reports financial support was provided by Engineering

and Physical Sciences Research Council. If there are other authors, they declare that they have no known competing financial interests or personal relationships that could have appeared to influence the work reported in this paper.

Data availability

Illumina Miseq data available under GeneBank accession: PRJNA1079668. Raw data available in Supplementary Table 10. R codes for AOB databse construction: https://github.com/Fchlt/ARC.

Acknowledgments

We would like to the University of LaRochelle and the LIENSs laboratory for hosting FC and CS as guest researchers and for providing access to their research facilities during the course of this study: the cytometry and imaging platform, the microbiology and molecular biology platforms and the 'logistic, field' facilities. We thank Laureen Beaugeard for the help during the cytometry analysis. This work was supported through a University of Glasgow College of Science and Engineering Doctoral studentship and the research exchange with the University of LaRochelle was supported by a research student mobility grant from the University of Glasgow and a research visit grant from the Microbiology Society. The work was also supported through a Science Foundation Ireland Starting Investigator Award (11/SIRG/B2159) a Royal Academy of Engineering (RAEng) Scottish Water Research Chair (RSF1718943) and an Engineering and Physical Sciences Research Council (EPSRC) award (Grant No. EP/V030515/1).

Appendix A. Supplementary data

Supplementary data to this article can be found online at https://doi.org/10.1016/j.scitotenv.2024.174312.

References

Agardy, T., Alder, J., Dayton, P., Curran, S., Kitchingman, A., Wilson, M., Catenazzi, A., Restrepo, J., Birkeland, C., Blaber, S., Saifullah, S., Branch, G., Boersma, D., Nixon, S., Dugan, P., Davidson, N., Vörösmarty, C., 2005. Coastal Systems. Current Status and Trends, Ecosystems and Human Well-being, pp. 513–550.

Alves, R.J.E., Wanek, W., Zappe, A., Richter, A., Svenning, M.M., Schleper, C., Urich, T., 2013. Nitrification rates in Arctic soils are associated with functionally distinct populations of ammonia-oxidizing archaea. ISME J. 7, 1620–1631. https://doi.org/10.1038/ismej.2013.35.

Alves, R.J.E., Minh, B.Q., Urich, T., von Haeseler, A., Schleper, C., 2018. Unifying the global phylogeny and environmental distribution of ammonia-oxidising archaea based on amoA genes. Nat. Commun. 9, 1517. https://doi.org/10.1038/s41467-018-03861-1.

Bergeon, L., Azémar, F., Carré, C., Dubillot, B., Emery, C., Agogué, H., Pineau, P., Lacoue-Labarthe, T., Bouvy, M., Tackx, M., Dupuy, C., 2023. Distribution and trophic functioning of planktonic communities in coastal marshes in Atlantic Coast of France. Estuar. Coast. Shelf Sci. 291 https://doi.org/10.1016/j.ecss.2023.108430.

Bernhard, A.E., Tucker, J., Giblin, A.E., Stahl, D.A., 2007. Functionally distinct communities of ammonia-oxidizing bacteria along an estuarine salinity gradient. Environ. Microbiol. 9, 1439–1447. https://doi.org/10.1111/j.1462-2920.2007.01260.x.

Blanchard, G.F., Paterson, D.M., Stal, L.J., Richard, P., Galois, R., Huet, V., Kelly, J., Honeywill, C., De Brouwer, J., Dyer, K., Christie, M., Seguignes, M., 2000. The effect of geomorphological structures on potential biostabilisation by microphytobenthos on intertidal mudflats. Cont. Shelf Res. 20, 1243–1256. https://doi.org/10.1016/S0278-4343(00)00021-2.

Bowen, J.L., Babbin, A.R., Kearns, P.J., Ward, B.B., 2014. Connecting the dots: linking nitrogen cycle gene expression to nitrogen fluxes in marine sediment mesocosms. Front. Microbiol. 5 https://doi.org/10.3389/fmicb.2014.00429.

Caffrey, J.M., Bano, N., Kalanetra, K., Hollibaugh, J.T., 2007. Ammonia oxidation and ammonia-oxidizing bacteria and archaea from estuaries with differing histories of hypoxia. ISME J. 1, 660–662. https://doi.org/10.1038/ismej.2007.79.

Callahan, B.J., McMurdie, P.J., Rosen, M.J., Han, A.W., Johnson, A.J.A., Holmes, S.P., 2016. DADA2: high-resolution sample inference from Illumina amplicon data. Nat. Methods 13, 581–583. https://doi.org/10.1038/nmeth.3869.

Callahan, B.J., McMurdie, P.J., Holmes, S.P., 2017. Exact sequence variants should replace operational taxonomic units in marker-gene data analysis. ISME J. 11, 2639–2643. https://doi.org/10.1038/ismej.2017.119.

Carling, P.A., Williams, J.J., Croudace, I.W., Amos, C.L., 2009. Formation of mud ridge and runnels in the intertidal zone of the Severn estuary, UK. Cont. Shelf Res. 29, 1913–1926. https://doi.org/10.1016/j.csr.2008.12.009.

Chang, Y., Fan, J., Su, J., Ming, H., Zhao, W., Shi, Y., Ji, F., Guo, L., Zan, S., Li, B., Guo, H., Guan, D., 2017. Spatial abundance, diversity, and activity of Ammonia-oxidizing Bacteria in coastal sediments of the Liaohe estuary. Curr. Microbiol. 74, 632–640. https://doi.org/10.1007/s00284-017-1226-x.

Cholet, F., Ijaz, U.Z., Smith, C.J., 2019. Differential ratio amplicons (R amp) for the evaluation of RNA integrity extracted from complex environmental samples. Environ. Microbiol. 21, 827–844. https://doi.org/10.1111/1462-2920.14516.

Cholet, F., Ijaz, U.Z., Smith, C.J., 2020. Reverse transcriptase enzyme and priming strategy affect quantification and diversity of environmental transcripts. Environ. Microbiol. 22, 2383–2402. https://doi.org/10.1111/1462-2920.15017.

Cholet, F., Lisik, A., Agogué, H., Ijaz, U.Z., Pineau, P., Lachaussée, N., Smith, C.J., 2022. Ecological Observations Based on Functional Gene Sequencing Are Sensitive to the Amplicon Processing Method, p. mSphere 7. https://doi.org/10.1128/msphere.00324-22.

Coskuner, G., Ballinger, S.J., Davenport, R.J., Pickering, R.L., Solera, R., Head, I.M., Curtis, T.P., 2005. Agreement between theory and measurement in quantification of ammonia-oxidizing bacteria. Appl. Environ. Microbiol. 71, 6325–6334. https://doi.org/10.1128/AEM.71.10.6325-6334.2005.

Costanza, R., de Groot, R., Sutton, P., van der Ploeg, S., Anderson, S.J., Kubiszewski, I., Farber, S., Turner, R.K., 2014. Changes in the global value of ecosystem services. Glob. Environ. Chang. 26, 152–158. https://doi.org/10.1016/j.gloenvcha.2014.04.002.

Daims, H., Lebedeva, E.V., Pjevac, P., Han, P., Herbold, C., Albertsen, M., Jehmlich, N., Palatinszky, M., Vierheilig, J., Bulaev, A., Kirkegaard, R.H., von Bergen, M., Rattei, T., Bendinger, B., Nielsen, P.H., Wagner, M., 2015. Complete nitrification by Nitrospira bacteria. Nature 528, 504–509. https://doi.org/10.1038/nature16461.

Daims, H., Lücker, S., Wagner, M., 2016. A new perspective on microbes formerly known as nitrite-oxidizing Bacteria. Trends Microbiol. 24, 699–712. https://doi.org/10.1016/j.tim.2016.05.004.

Damashek, J., Smith, J.M., Mosier, A.C., Francis, C.A., 2015. Benthic ammonia oxidizers differ in community structure and biogeochemical potential across a riverine delta. Front. Microbiol. 6, 1–18. https://doi.org/10.3389/fmicb.2014.00743.

Dimitri Kits, K., Sedlacek, C.J., Lebedeva, E.V., Han, P., Bulaev, A., Pjevac, P., Daebeler, A., Romano, S., Albertsen, M., Stein, L.Y., Daims, H., Wagner, M., 2017. Kinetic analysis of a complete nitrifier reveals an oligotrophic lifestyle. Nature 549, 269–272. https://doi.org/10.1038/nature23679.

Duff, A.M., Zhang, L.M., Smith, C.J., 2017. Small-scale variation of ammonia oxidisers within intertidal sediments dominated by ammonia-oxidising bacteria Nitrosomonas sp. amoA genes and transcripts. Sci. Rep. 7, 1–13. https://doi.org/10.1038/s41598-017-13583-x.

Fan, H., Bolhuis, H., Stal, L.J., 2015. Nitrification and nitrifying bacteria in a coastal microbial mat. Front. Microbiol. 6 https://doi.org/10.3389/fmicb.2015.01367.

Fowler, S.J., Palomo, A., Dechesne, A., Mines, P.D., Smets, B.F., 2018. *Comammox nitrospira* are abundant ammonia oxidizers in diverse groundwater-fed rapid sand filter communities. Environ. Microbiol. 20, 1002–1015. https://doi.org/10.1111/1462920.14033.

Francis, C.A., O'Mullan, G.D., Ward, B.B., 2003. Diversity of ammonia monooxygenase (amoA) genes across environmental gradients in Chesapeake Bay sediments. Geobiology 1, 129–140. https://doi.org/10.1046/j.1472-4669.2003.00010.x.

Gruber, N., Galloway, J.N., 2008. An earth-system perspective of the global nitrogen cycle. Nature 451, 293–296. https://doi.org/10.1038/nature06592.

He, H., Zhen, Y., Mi, T., Fu, L., Yu, Z., 2018. Ammonia-oxidizing archaea and bacteria differentially contribute to ammonia oxidation in sediments from adjacent waters of Rushan Bay. China. Front Microbiol 9. https://doi.org/10.3389/fmicb.2018.00116.

He, X., Ji, G., 2020. Responses of AOA and AOB activity and DNA/cDNA community structure to allylthiourea exposure in the water level fluctuation zone soil. Environ. Sci. Pollut. Res. 27, 15233–15244. https://doi.org/10.1007/s11356-020-07952-9.

Hommes, N.G., Sayavedra-Soto, L.A., Arp, D.J., 2003. Chemolithoorganotrophic growth of Nitrosomonas europaea on fructose. J. Bacteriol. 185, 6809–6814. https://doi.org/10.1128/JB.185.23.6809-6814.2003.

Hornek, R., Pommerening-Röser, A., Koops, H.P., 2006. Primers containing universal bases reduce multiple amoA gene specific DGGE band patterns when analysing the diversity of beta-ammonia oxidizers in the environment. J. Microbial Methods 66, 147–155.

Hou, L., Liu, M., Carini, S.A., Gardner, W.S., 2012. Transformation and fate of nitrate near the sediment-water interface of Copano Bay. Cont. Shelf Res. 35, 86–94. https://doi.org/10.1016/j.csr.2012.01.004.

Jian, C., Luukkonen, P., Yki-Järvinen, H., Salonen, A., Korpela, K., 2020. Quantitative PCR provides a simple and accessible method for quantitative microbiota profiling. PLoS One 15. https://doi.org/10.1371/journal.pone.0227285.

Kahle, D., Wickham, H., 2013. Ggmap: spatial visualization with ggplot2. R J 5 (1), 144–161.

van Kessel, M.A.H.J., Speth, D.R., Albertsen, M., Nielsen, P.H., Op den Camp, H.J.M., Kartal, B., Jetten, M.S.M., Lücker, S., 2015. Complete nitrification by a single microorganism. Nature 528, 555–559. https://doi.org/10.1038/nature16459.

Kool, D.M., Dolfing, J., Wrage, N., Van Groenigen, J.W., 2011. Nitrifier denitrification as a distinct and significant source of nitrous oxide from soil. Soil Biol. Biochem. 43, 174–178. https://doi.org/10.1016/j.soilbio.2010.09.030.

Laima, M., Brossard, D., Girard, M., Richard, P., Gouleau, D., Joassard, L., 2002. The influence of long emersion on biota, ammonium fluxes and nitrification in intertidal sediments of Marennes-Oléron Bay, France. Mar. Environ. Res. 53, 381–402.

Laima, M.J.C., Girard, M.F., Vouvé, F., Richard, P., Blanchard, G., Gouleau, D., 1999. Nitrification rates related to sedimentary structures in an Atlantic intertidal mudflat,

Marennes-Oleron Bay, France. Mar. Ecol. Prog. Ser. 191, 33–41. https://doi.org/10.3354/meps191033.
Lavergne, C., Beaugeard, L., Dupuy, C., Courties, C., Agogué, H., 2014. An efficient and rapid method for the enumeration of heterotrophic prokaryotes in coastal sediments by flow cytometry. J. Microbiol. Methods 105, 31–38. https://doi.org/10.1016/j.mimet.2014.07.002.
Lavergne, C., Agogué, H., Leynaert, A., Raimonet, M., De Wit, R., Pineau, P., Bréret, M., Lachaussée, N., Dupuy, C., 2017. Factors influencing prokaryotes in an intertidal mudflat and the resulting depth gradients. Estuar. Coast. Shelf Sci. 189, 74–83. https://doi.org/10.1016/j.ecss.2017.03.008.
Lavergne, C., Hugoni, M., Hubas, C., Debroas, D., Dupuy, C., Agogué, H., 2018. Diel rhythm does not shape the vertical distribution of bacterial and archaeal 16S rRNA transcript diversity in intertidal sediments: a Mesocosm study. Microb. Ecol. 75, 364–374. https://doi.org/10.1007/s00248-017-1048-1.
Li, J., Nedwell, D.B., Beddow, J., Dumbrell, A.J., McKew, B.A., Thorpe, E.L., Whitby, C., 2015. amoA gene abundances and nitrification potential rates suggest that benthic ammonia-oxidizing bacteria and not archaea dominate N cycling in the Colne estuary, United Kingdom. Appl. Environ. Microbiol. 81, 159–165. https://doi.org/10.1128/AEM.02654-14.
Li, M., He, H., Mi, T., Zhen, Y., 2022. Spatiotemporal dynamics of ammonia-oxidizing archaea and bacteria contributing to nitrification in sediments from Bohai Sea and South Yellow Sea. China. Science of the Total Environment 825. https://doi.org/10.1016/j.scitotenv.2022.153972.
Lin, H., Peddada, S. Das, 2020. Analysis of compositions of microbiomes with bias correction. Nat. Commun. 11 https://doi.org/10.1038/s41467-020-17041-7.
Lipsewers, Y.A., Bale, N.J., Hopmans, E.C., Schouten, S., Sinninghe Damsté, J.S., Villanueva, L., 2014. Seasonality and depth distribution of the abundance and activity of ammonia oxidizing microorganisms in marine coastal sediments (North Sea). Front. Microbiol. 5 https://doi.org/10.3389/fmicb.2014.00472.
Liu, H., Zhou, P., Cheung, S., Lu, Y., Liu, Hongbin, Jing, H., 2022. Distribution and oxidation rates of Ammonia-oxidizing Archaea influenced by the coastal upwelling off eastern Hainan Island. Microorganisms 10. https://doi.org/10.3390/microorganisms10050952.
Liu, T., Yang, H., 2021. An RNA-based study of the distribution of ammonia-oxidizing microorganisms in vertical sediment. Ecol. Indic. 121 https://doi.org/10.1016/j.ecolind.2020.10714.
Lorenzent, C.J., 1966. A method for the continuous measurement of in vivo chlorophyll concentration. In: Deep-Sea Research 13, 223–227. Pergamon Press, Ltd.
Marshall, A.J., Phillips, L., Longmore, A., Hayden, H.L., Heidelberg, K.B., Tang, C., Mele, P., 2023. Temporal profiling resolves the drivers of microbial nitrogen cycling variability in coastal sediments. Sci. Total Environ. 856 https://doi.org/10.1016/j.scitotenv.2022.159057.
Marton, J.M., Roberts, B.J., Bernhard, A.E., Giblin, A.E., 2015. Spatial and temporal variability of nitrification potential and Ammonia-oxidizer abundances in Louisiana salt marshes. Estuar. Coasts 38, 1824–1837. https://doi.org/10.1007/s12237-015-9943-5.
Mosier, A.C., Francis, C.A., 2008. Relative abundance and diversity of ammonia-oxidizing archaea and bacteria in the San Francisco Bay estuary. Environ. Microbiol. 10, 3002–3016. https://doi.org/10.1111/j.1462-2920.2008.01764.x.
Oksanen, J., Kindt, R., O'Hara, R.B., 2005. Vegan: community ecology package. Available from http://cc.oulu.fi/~jarioksa/ 3.
O'Mullan, G.D., Ward, B.B., 2005. Relationship of temporal and spatial variabilities of ammonia-oxidizing bacteria to nitrification rates in Monterey Bay, California. Appl. Environ. Microbiol. 71, 697–705. https://doi.org/10.1128/AEM.71.2.697-705.2005.
Peng, X., Yando, E., Hildebrand, E., Dwyer, C., Kearney, A., Waciega, A., Valiela, I., Bernhard, A.E., 2012. Differential responses of ammonia-oxidizing archaea and bacteria to long-term fertilization in a New England salt marsh. Front. Microbiol. 3, 1–11. https://doi.org/10.3389/fmicb.2012.00445.
Prosser, J.I., Hink, L., Gubry-Rangin, C., Nicol, G.W., 2020. Nitrous oxide production by ammonia oxidizers: physiological diversity, niche differentiation and potential mitigation strategies. Glob. Chang. Biol. https://doi.org/10.1111/gcb.14877.
R Core Team, 2021. R: A language and environment for statistical computing. R Foundation for Statistical Computing, Vienna, Austria. https://www.R-project.org/.
Sanders, T., Laanbroek, H.J., 2018. The distribution of sediment and water column nitrification potential in the hyper-turbid ems estuary. Aquat. Sci. 80 https://doi.org/10.1007/s00027-018-0584-1.
Santoro, A.E., Francis, C.A., De Sieyes, N.R., Boehm, A.B., 2008. Shifts in the relative abundance of ammonia-oxidizing bacteria and archaea across physicochemical gradients in a subterranean estuary. Environ. Microbiol. 10, 1068–1079. https://doi.org/10.1111/j.1462-2920.2007.01547.x.
Santos, J.P., Mendes, D., Monteiro, M., Ribeiro, H., Baptista, M.S., Borges, M.T., Magalhães, C., 2018. Salinity impact on ammonia oxidizers activity and amoA expression in estuarine sediments. Estuar. Coast. Shelf Sci. 211, 177–187. https://doi.org/10.1016/j.ecss.2017.09.001.
Seitz, R.D., Wennhage, H., Bergstrom, U., Lipcius, R.N., Ysebaert, T., 2014. Ecological value of coastal habitats for commercially and ecologically important species. ICES J. Mar. Sci. 71, 648–665.
Seitzinger, S.P., Harrison, J.A., Böhlke, J.K., Bouwman, A.F., Lowrance, R., Tobias, C., Drecht, G. Van, 2006. Denitrification across landscapes and waterscapes : a synthesis. Ecol. Appl. 16, 2064–2090.
Smith, J.M., Mosier, A.C., Francis, C.A., 2015. Spatiotemporal relationships between the abundance, distribution, and potential activities of Ammonia-oxidizing and denitrifying microorganisms in intertidal sediments. Microb. Ecol. 69, 13–24. https://doi.org/10.1007/s00248-014-0450-1.
Su, Y., Wang, W., Wu, D., Huang, W., Wang, M., Zhu, G., 2018. Stimulating ammonia oxidizing bacteria (AOB) activity drives the ammonium oxidation rate in a constructed wetland (CW). Sci. Total Environ. 624, 87–95. https://doi.org/10.1016/j.scitotenv.2017.12.084.
Suzuki, M.T., Taylor, L.T., Delong, E.F., Long, E.F.D.E., 2000. Quantitative Analysis of Small-Subunit rRNA Genes in Mixed Microbial Populations Via 5′-Nuclease Assays Quantitative Analysis of Small-Subunit rRNA Genes in Mixed Microbial Populations Via 5 J -Nuclease Assays 66, 4605–4614. https://doi.org/10.1128/AEM.66.11.4605-4614.2000.Updated.
Tatti, E., Duff, A.M., Kostrytsia, A., Cholet, F., Ijaz, U.Z., Smith, C.J., 2022. Potential nitrification activity reflects ammonia oxidizing bacteria but not archaea activity across a soil-sediment gradient. Estuar. Coast. Shelf Sci. 264, 107666 https://doi.org/10.1016/j.ecss.2021.107666.
Tettamanti Boshier, F.A., Srinivasan, S., Lopez, A., Hoffman, N.G., Proll, S., Fredricks, D. N., Schiffer, J.T., 2020. Complementing 16S rRNA gene amplicon sequencing with Total bacterial load to infer absolute species concentrations in the vaginal microbiome. mSystems 5. doi:https://doi.org/10.1128/msystems.00777-19.
Urakawa, H., Martens-Habbena, W., Huguet, C., de la Torre, J.R., Ingalls, A.E., Devol, A. H., Stahl, D.A., 2014. Ammonia availability shapes the seasonal distribution and activity of archaeal and bacterial ammonia oxidizers in the Puget Sound estuary. Limnol. Oceanogr. 59, 1321–1335. https://doi.org/10.4319/lo.2014.59.4.1321.
Walters, W.R.Hyde E., Berg-Lyons, D., Ackermann, G., Humphrey, G., Parada, A., Gilbert, J.A., Jansson, J.K., Caporaso, J.G., Fuhrman, J.A., Apprill, A., Knightb, R., 2015. Improved Bacterial 16S rRNA Gene (V4 and V4–5) and Fungal Internal Transcribed Spacer Marker Gene Primers for Microbial Community Surveys. mSystems 1, 1–10. https://doi.org/10.1128/mSystems.00009-15. Editor.
Wang, C., Tang, S., He, X., Ji, G., 2020. The abundance and community structure of active ammonia-oxidizing archaea and ammonia-oxidizing bacteria shape their activities and contributions in coastal wetlands. Water Res. 171 https://doi.org/10.1016/j.watres.2019.115464.
Wankel, S.D., Mosier, A.C., Hansel, C.M., Paytan, A., Francis, C.A., 2011. Spatial variability in nitrification rates and ammonia-oxidizing microbial communities in the agriculturally impacted Elkhorn Slough estuary, California. Appl. Environ. Microbiol. 77, 269–280. https://doi.org/10.1128/AEM.01318-10.
Wickham, H., 2016. ggplot2 Elegant Graphics for Data Analysis, Second edition. Springer International Publishing.
Wright, C.L., Lehtovirta-Morley, L.E., 2023. Nitrification and beyond: metabolic versatility of ammonia oxidising archaea. ISME J. https://doi.org/10.1038/s41396-023-01467-0.
Wuchter, C., Abbas, B., Coolen, M.J.L., Herfort, L., van Bleijswijk, J., Timmers, P., Strous, M., Teira, E., Herndl, G.J., Middelburg, J.J., Schouten, S., Sinninghe Damste, J.S., 2006. Archaeal nitrification in the ocean. Proc. Natl. Acad. Sci. 103, 12317–12322. https://doi.org/10.1073/pnas.0600756103.
Zhang, L.M., Duff, A.M., Smith, C.J., 2018. Community and functional shifts in ammonia oxidizers across terrestrial and marine (soil/sediment) boundaries in two coastal bay ecosystems. Environ. Microbiol. 20, 2834–2853. https://doi.org/10.1111/1462-2920.14238.
Zhang, Y., Chen, L., Dai, T., Sun, R., Wen, D., 2015a. Ammonia manipulates the ammonia-oxidizing archaea and bacteria in the coastal sediment-water microcosms. Appl. Microbiol. Biotechnol. 99, 6481–6491. https://doi.org/10.1007/s00253-015-6524-2.
Zhang, Y., Chen, L., Dai, T., Tian, J., Wen, D., 2015b. The influence of salinity on the abundance, transcriptional activity, and diversity of AOA and AOB in an estuarine sediment: a microcosm study. Appl. Microbiol. Biotechnol. 99, 9825–9833. https://doi.org/10.1007/s00253-015-6804-x.